

Biophysics. In the article “Folding and aggregation of designed proteins” by R. A. Broglia, G. Tiana, S. Pasquali, H. E. Roman, and E. Vigezzi, which appeared in number 22, October 27, 1998, of *Proc. Natl. Acad. Sci. USA* (**95**, 12930–12933), the following correction should be noted. In Fig. 1*b*, the designed sequence of amino acids S₃₆ contains a typographical error in that only 35 of its 36 monomers appear. The missing amino acid is of type R and should be located between amino acids E (sixth) and G (seventh). The correct sequence is:

S₃₆ = SQKWLERGATRIADGDLPVNGTYFSCKIMENVHPLA.

Although this typographical error does not change the results presented in the paper because they were obtained with the correct number and sequence of amino acids, it constitutes a nuisance for anybody interested in reproducing our results, and we apologize for the inconvenience. We want to thank Prof. H. S. Chan, of the University of Toronto, for calling our attention to this error.

Cell Biology. In the article “Quantitative analysis of biological membrane lipids at the low picomole level by nano-electrospray ionization tandem mass spectrometry” by B. Brügger, G. Erben, R. Sandhoff, F. T. Wieland, and W. D.

Genetics. In the article “Cluster analysis and display of genome-wide expression patterns” by Michael B. Eisen, Paul T. Spellman, Patrick O. Brown, and David Botstein, which appeared in number 25, December 8, 1998, of *Proc. Natl. Acad. Sci. USA* (**95**, 14863–14868), the authors want to note that two references were inadvertently omitted. Ref. 1 refers to a precedent for coloring of data tables following cluster analysis, and ref. 2 refers to an earlier example of applying cluster analysis to gene expression data. The additional references are:

1. Weinstein, J. N., Myers, T. G., O'Connor, P. M., Friend, S. H., Fornace, A. J., Jr., Kohn, K. W., Fojo, T., Bates, S. E., Rubinstein, L. V., Anderson, N. L., *et al.* (1997) *Science* **275**, 343–349.
2. Wen, X., Fuhrman, S., Michaels, G. S., Carr, D. B., Smith, S., Barker, J. L. & Somogyi, R. (1998) *Proc. Natl. Acad. Sci. USA* **95**, 334–339.

Lehmann, which appeared in number 6, March 18, 1997, of *Proc. Natl. Acad. Sci. USA* (**94**, 2339–2344), Table 1 contains errors. A corrected table is reprinted below with corrections in boldface type.

Table 1. Identification of the most abundant signals in the ESI mass spectra of total lipid extract of CHO cells, as given in Fig. 1*a* and *b*

Class of phospholipid	Ion	Total fatty acid carbon no.:no. of double bonds								
		32:1	34:2	36:2	38:4	16:0	18:0	22:0	24:1	26:0
PA	[M-H] ⁻	645	671	699	723					
PS	[M-H] ⁻	732	758	786	810					
PE	[M-H] ⁻	688	714	742	766					
Plasmenyl-PE	[M-H] ⁻	672	698	726	750					
PI	[M-H] ⁻	807	833	861	885					
PG	[M-H] ⁻	719	745	773	797					
PC	[M+H] ⁺	732	758	786	810					
	[M+Na] ⁺	754	780	808	832					
Plasmenyl-PC	[M+H] ⁺	716	742	770	794					
	[M+Na] ⁺	738	764	792	816					
PE	[M+H] ⁺	690	716	744	768					
Plasmenyl-PE	[M+H] ⁺	674	700	728	752					
PS	[M+H] ⁺	734	760	788	812					
SM	[M+H] ⁺					703	731	787	813	843
	[M+Na] ⁺					725	753	809	835	865

In the negative ion mode, PS and PE (with two nitrogen atoms) show signals at even-numbered *m/z* values, whereas PI, PG, and PA show signals at odd-numbered values. In the positive ion mode, SM signals appear at odd *m/z* values (2 nitrogen atoms), whereas PC, PE, and PS-signals occur at even *m/z* values. The *m/z* values are nominal monoisotopic data.

Genetics. In the article “Neurosecretory control of aging in *Caenorhabditis elegans*” by Michael Ailion, Takao Inoue, Carole I. Weaver, Robert W. Holdcraft, and James H. Thomas, which appeared in number 13, June 22, 1999, of *Proc. Natl. Acad. Sci. USA* (96, 7394–7397), the following corrections should be noted.

(i) Figs. 1 and 2 were interchanged. The figure legends are correct, but the figures were transposed. The corrected figures and their legends are shown below. (ii) In Table 2, line 2, the genotype of the strain should be *unc-64(e246)*, not *unc-63(e246)*. (iii) Table 1 originally had blank lines separating the top, middle, and bottom sections of the table. Without these spaces, it is difficult to tell what is referred to as top, middle, and bottom in the table legend. Top refers to lines 1–6, middle refers to lines 7–8, and bottom refers to lines 9–12.

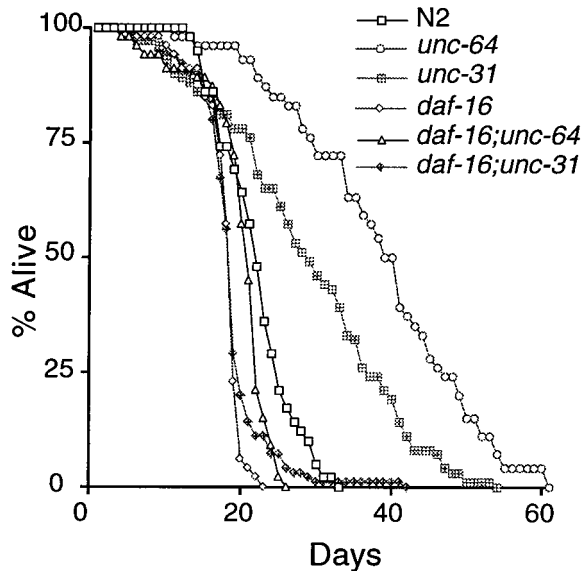


FIG. 1. *unc-64* and *unc-31* mutants have increased life spans and are suppressed by *daf-16*. Assays were performed at 20°. *unc-64* and *unc-31* have significantly longer life spans than N2 ($P < 0.0001$ for *unc-64* and $P = 0.0004$ for *unc-31*). This figure uses the same data set as Table 1.

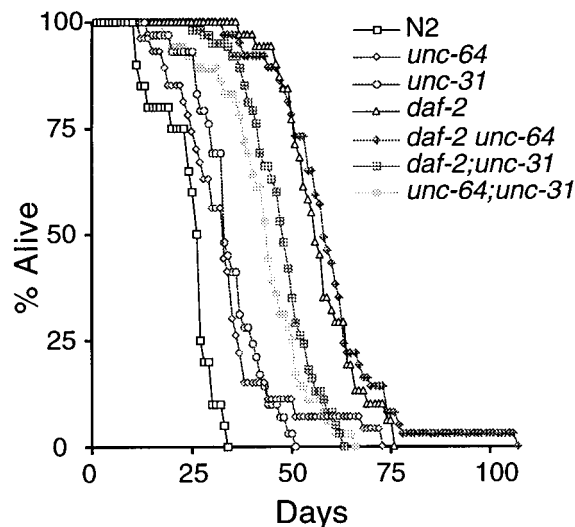


FIG. 2. Mutations in *unc-64* and *unc-31* do not enhance the longevity of *daf-2* mutants. Animals were grown at 15° to allow development past the dauer stage and then were shifted to 20°. *unc-64*; *unc-31* had a significantly longer life span than either *unc-64* ($P = 0.0002$) or *unc-31* ($P = 0.0005$). The *daf-2 unc-64* double mutant and *daf-2* were not significantly different ($P = 0.5139$). The maximum life span of *daf-2 unc-64* was extended to >100 days by a single animal. We have not investigated whether this has any possible significance. This figure uses the same data set as Table 2.

Medical Sciences. In the article “Osteopontin-deficient mice are resistant to ovariectomy-induced bone resorption” by Hiroyuki Yoshitake, Susan R. Rittling, David T. Denhardt, and Masaki Noda, which appeared in number 14, July, 1999, of *Proc. Natl. Acad. Sci. USA* (96, 8156–8160), the authors request the following correction. In the 9th line in the first paragraph and in Table 3 on page 8158, the unit in the text and the third subheading under Parameters in the table are incorrectly listed as BFR/BV, $\mu\text{m}^3/\mu\text{m}^2/\text{day}$. The correct listing is BFR/BV, %/year.

Medical Sciences. In the article “Cancer-specific chromosome alterations in the constitutive fragile region *FRA3B*” by Koshi Mimori, Teresa Druck, Hiroshi Inoue, Hansjuerg Alder, Lori Berk, Masaki Mori, Kay Huebner, and Carlo M. Croce, which appeared in number 13, June 22, 1999, of *Proc. Natl. Acad. Sci. USA* 96, 7456–7461, the following correction should be noted. *FHIT* exon 4 was misplaced in Figs. 1 and 2. Its true placement is ≈ 40 kilobase pairs further centromeric at base pairs 162581 to 162673 of GenBank submission AF152363. Thus, the length of intron 4 is 284935 base pairs and the markers D3S4489 and D3S4260 and the proximal aphidicolin-induced hybrid breaks are telomeric to exon 4, i.e., in intron 4.

Microbiology. In the article “A set of independent selectable markers for transfection of the human malaria parasite *Plasmodium falciparum*” by Choukri Ben Mamoun, Ilya Y. Gluzman, Sophie Goyard, Stephen M. Beverley, and Daniel E. Goldberg, which appeared in number 15, July 20, 1999, of *Proc. Natl. Acad. Sci. USA* (96, 8716–8720), the authors request the following corrections. In *Experimental Procedures* (page 8717), under “*P. falciparum* Transfection and Selection of Transfectants,” there was a typographical error in the concentrations of G418 used for selection. The correct concentrations are 300, 500, or 1,000 $\mu\text{g}/\text{ml}$. Under “BSD Enzyme Assay,” there was a typographical error in the volume of cultured parasitized red blood cells used. The correct volume is 12 ml. In *Results* (page 8718, line 24 in column 2), the sentence should read: “Varying amounts of either gene were slotted onto the blot, corresponding to the amount of DNA that would be present per microgram of total DNA if there were 1–35 copies of the construct per cell.”

Neurobiology. In the article “Bilirubin, formed by activation of heme oxygenase-2, protects neurons against oxidative stress injury” by Sylvain Doré, Masaaki Takahashi, Christopher D. Ferris, Lynda D. Hester, Daniel Guastella, and Solomon H. Snyder, which appeared in number 5, March 2, 1999, of *Proc. Natl. Acad. Sci. USA* (96, 2445–2450), the authors request the following correction. One of the authors, Randa Zakhary, was deleted from the final published paper. The correct author and affiliation lines are as follows:

SYLVAIN DORÉ*, MASAOKI TAKAHASHI*, CHRISTOPHER D. FERRIS*†, RANDA ZAKHARY*, LYNDY D. HESTER*, DANIEL GUASTELLA*, AND SOLOMON H. SNYDER*‡§¶

Departments of *Neuroscience, †Pharmacology and Molecular Sciences, ‡Medicine, and §Psychiatry, The Johns Hopkins University School of Medicine, 725 North Wolfe Street, Baltimore, MD 21205

Cluster analysis and display of genome-wide expression patterns

MICHAEL B. EISEN*, PAUL T. SPELLMAN*, PATRICK O. BROWN†, AND DAVID BOTSTEIN*‡

*Department of Genetics and †Department of Biochemistry and Howard Hughes Medical Institute, Stanford University School of Medicine, 300 Pasteur Avenue, Stanford, CA 94305

Contributed by David Botstein, October 13, 1998

ABSTRACT A system of cluster analysis for genome-wide expression data from DNA microarray hybridization is described that uses standard statistical algorithms to arrange genes according to similarity in pattern of gene expression. The output is displayed graphically, conveying the clustering and the underlying expression data simultaneously in a form intuitive for biologists. We have found in the budding yeast *Saccharomyces cerevisiae* that clustering gene expression data groups together efficiently genes of known similar function, and we find a similar tendency in human data. Thus patterns seen in genome-wide expression experiments can be interpreted as indications of the status of cellular processes. Also, coexpression of genes of known function with poorly characterized or novel genes may provide a simple means of gaining leads to the functions of many genes for which information is not available currently.

The rapid advance of genome-scale sequencing has driven the development of methods to exploit this information by characterizing biological processes in new ways. The knowledge of the coding sequences of virtually every gene in an organism, for instance, invites development of technology to study the expression of all of them at once, because the study of gene expression of genes one by one has already provided a wealth of biological insight. To this end, a variety of techniques has evolved to monitor, rapidly and efficiently, transcript abundance for all of an organism's genes (1–3). Within the mass of numbers produced by these techniques, which amount to hundreds of data points for thousands or tens of thousands of genes, is an immense amount of biological information. In this paper we address the problem of analyzing and presenting information on this genomic scale.

A natural first step in extracting this information is to examine the extremes, e.g., genes with significant differential expression in two individual samples or in a time series after a given treatment. This simple technique can be extremely efficient, for example, in screens for potential tumor markers or drug targets. However, such analyses do not address the full potential of genome-scale experiments to alter our understanding of cellular biology by providing, through an inclusive analysis of the entire repertoire of transcripts, a continuing comprehensive window into the state of a cell as it goes through a biological process. What is needed instead is a holistic approach to analysis of genomic data that focuses on illuminating order in the entire set of observations, allowing biologists to develop an integrated understanding of the process being studied.

A natural basis for organizing gene expression data is to group together genes with similar patterns of expression. The first step to this end is to adopt a mathematical description of similarity. For any series of measurements, a number of sensible measures of similarity in the behavior of two genes can

be used, such as the Euclidean distance, angle, or dot products of the two n -dimensional vectors representing a series of n measurements. We have found that the standard correlation coefficient (i.e., the dot product of two normalized vectors) conforms well to the intuitive biological notion of what it means for two genes to be “coexpressed;” this may be because this statistic captures similarity in “shape” but places no emphasis on the magnitude of the two series of measurements.

It is not the purpose of this paper to survey the various methods available to cluster genes on the basis of their expression patterns, but rather to illustrate how such methods can be useful to biologists in the analysis of gene expression data. We aim to use these methods to organize, but not to alter, tables containing primary data; we have thus used methods that can be reduced, in the end, to a reordering of lists of genes. Clustering methods can be divided into two general classes, designated supervised and unsupervised clustering (4). In supervised clustering, vectors are classified with respect to known reference vectors. In unsupervised clustering, no pre-defined reference vectors are used. As we have little *a priori* knowledge of the complete repertoire of expected gene expression patterns for any condition, we have favored unsupervised methods or hybrid (unsupervised followed by supervised) approaches.

Although various clustering methods can usefully organize tables of gene expression measurements, the resulting ordered but still massive collection of numbers remains difficult to assimilate. Therefore, we always combine clustering methods with a graphical representation of the primary data by representing each data point with a color that quantitatively and qualitatively reflects the original experimental observations. The end product is a representation of complex gene expression data that, through statistical organization and graphical display, allows biologists to assimilate and explore the data in a natural intuitive manner.

To illustrate this approach, we have applied pairwise average-linkage cluster analysis (5) to gene expression data collected in our laboratories. This method is a form of hierarchical clustering, familiar to most biologists through its application in sequence and phylogenetic analysis. Relationships among objects (genes) are represented by a tree whose branch lengths reflect the degree of similarity between the objects, as assessed by a pairwise similarity function such as that described above. In sequence comparison, these methods are used to infer the evolutionary history of sequences being compared. Whereas no such underlying tree exists for expression patterns of genes, such methods are useful in their ability to represent varying degrees of similarity and more distant relationships among groups of closely related genes, as well as in requiring few assumptions about the nature of the data. The computed trees can be used to order genes in the original data table, so that genes or groups of genes with similar expression patterns are adjacent. The ordered table can then be displayed graphically, as above, with a representation of the tree to indicate the relationships among genes.

The publication costs of this article were defrayed in part by page charge payment. This article must therefore be hereby marked “advertisement” in accordance with 18 U.S.C. §1734 solely to indicate this fact.

© 1998 by The National Academy of Sciences 0027-8424/98/9514863-6\$2.00/0
PNAS is available online at www.pnas.org.

‡To whom reprint requests should be addressed. e-mail: botstein@genome.stanford.edu.

MATERIALS AND METHODS

Sources of Experimental Data. Data analyzed here were collected on spotted DNA microarrays (6, 7). Gene expression in the budding yeast *Saccharomyces cerevisiae* was studied during the diauxic shift (8), the mitotic cell division cycle (9), sporulation (10), and temperature and reducing shocks (P.T.S., P.O.B., and D.B., unpublished results) by using microarrays containing essentially every ORF from this fully sequenced organism (8). Gene expression of primary human fibroblasts stimulated with serum following serum starvation was studied by using a microarray with 9,800 cDNAs representing approximately 8,600 distinct human transcripts (11). In all experiments, RNA from experimental samples (taken at selected times during the process) was labeled during reverse transcription with the red-fluorescent dye Cy5 (Amersham) and was mixed with a reference sample labeled in parallel with the green-fluorescent dye Cy3 (Amersham) (the reference sample was time 0 for all experiments, except for the yeast cell cycle where asynchronous cells were used). After hybridization and appropriate washing steps, separate images were acquired for each fluor, and fluorescence intensity ratios were obtained for all target elements.

We maintain and update master data tables for all experiments conducted in our labs; in these tables, rows represent all genes for which data has been collected, columns represent individual array experiments (e.g., single timepoints or conditions), and each cell represents the measured Cy5/Cy3 fluorescence ratio at the corresponding target element on the appropriate array. All ratio values are log transformed (base 2 for simplicity) to treat inductions or repressions of identical magnitude as numerically equal but with opposite sign. Individual observations are rejected in some cases, on the basis of measurement quality parameters produced by the image analysis software. For the analyses presented here, smaller tables containing selected genes and experiments were produced; full descriptions are given in the appropriate figure legends. These tables are available on the PNAS web site at (www.pnas.org) or at <http://rana.stanford.edu/clustering>.

Metrics. The gene similarity metric we use is a form of correlation coefficient. Let G_i equal the (log-transformed) primary data for gene G in condition i . For any two genes X and Y observed over a series of N conditions, a similarity score can be computed as follows:

$$S(X, Y) = \frac{1}{N} \sum_{i=1, N} \left(\frac{X_i - X_{offset}}{\Phi_X} \right) \left(\frac{Y_i - Y_{offset}}{\Phi_Y} \right)$$

where

$$\Phi_G = \sqrt{\sum_{i=1, N} \frac{(G_i - G_{offset})^2}{N}}$$

When G_{offset} is set to the mean of observations on G , then Φ_G becomes the standard deviation of G , and $S(X, Y)$ is exactly equal to the Pearson correlation coefficient of the observations of X and Y . Values of G_{offset} which are not the average over observations on G are used when there is an assumed unchanged or reference state represented by the value of G_{offset} , against which changes are to be analyzed; in all of the examples presented here, G_{offset} is set to 0, corresponding to a fluorescence ratio of 1.0.

Hierarchical Clustering. The hierarchical clustering algorithm used is based closely on the average-linkage method of Sokal and Michener (5), which was developed for clustering correlation matrixes such as those used here. The object of this algorithm is to compute a dendrogram that assembles all elements into a single tree. For any set of n genes, an upper-diagonal similarity matrix is computed by using the metric described above, which contains similarity scores for all

pairs of genes. The matrix is scanned to identify the highest value (representing the most similar pair of genes). A node is created joining these two genes, and a gene expression profile is computed for the node by averaging observation for the joined elements (missing values are omitted and the two joined elements are weighted by the number of genes they contain). The similarity matrix is updated with this new node replacing the two joined elements, and the process is repeated $n-1$ times until only a single element remains. Software implementation of this algorithm can be obtained from the authors at <http://rana.stanford.edu/clustering>.

Ordering of Data Tables. For any dendrogram of n elements, there are 2^{n-1} linear orderings consistent with the structure of the tree (at each node, either of the two elements joined by the node can be ordered ahead of the other). An optimal linear ordering, one that maximizes the similarity of adjacent elements in the ordering, is impractical to compute. However, to consistently arrange nodes between analyses, we use simple methods of weighting genes, such as average expression level, time of maximal induction, or chromosomal position, and we place the element with the lower average weight earlier in the final ordering.

Display. Using any ordering, the primary data table is represented graphically by coloring each cell on the basis of the measured fluorescence ratio. Cells with log ratios of 0 (ratios of 1.0 – genes unchanged) are colored black, increasingly positive log ratios with reds of increasing intensity, and increasingly negative log ratios with greens of increasing intensity. A representation of the dendrogram is appended to the colored table to indicate the nature of the computed relationship among genes in the table.

RESULTS

We applied this method to two sets of data, a single time course (Fig. 1) of a canonical model of the growth response in human cells (11) and an aggregation of data from experiments on the budding yeast *S. cerevisiae* (Fig. 2), including time courses of the mitotic cell division cycle (9), sporulation (10), the diauxic shift (8), and shock responses (P.T.S., P.O.B., and D.B., unpublished results). A striking property of the clustered images in Figs. 1 and 2 is the presence of large contiguous patches of color representing groups of genes that share similar expression patterns over multiple conditions. To verify that this structure is of biological origin and is not an artifact of the clustering procedure, the initial data from the human growth response experiment were randomized in three different ways and were clustered by using the same procedure (Fig. 3). No similar structure resulted from any of these randomized data sets, indicating that the patterns seen in Figs. 1 and 2 depict biological order in the gene expression response of the organism during the studied processes.

A central feature of Figs. 1 and 2 is that one can look at such images, identify patterns of interest, and readily zoom in on the detailed expression patterns and identities of the genes contributing to these patterns. An important test of the value of this approach comes when we examine the identity of the clustered genes at varying levels of identity.

Redundant Representations of Genes Cluster Together. At the finest level, we have found repeatedly that genes represented by more than one array element or genes with high degrees of sequence identity are clustered next to, or in the immediate vicinity of, each other. Thus the exact representation of a gene on the array (alternate cDNA clones of differing length in the case of human arrays or highly homologous genes in *S. cerevisiae*) makes little difference in the observed pattern of gene expression. Moreover, even though groups of genes may show very similar patterns of expression, as is seen in Figs. 1 and 2, in general individual genes can be distinguished from all other genes on the basis of subtle differences in their

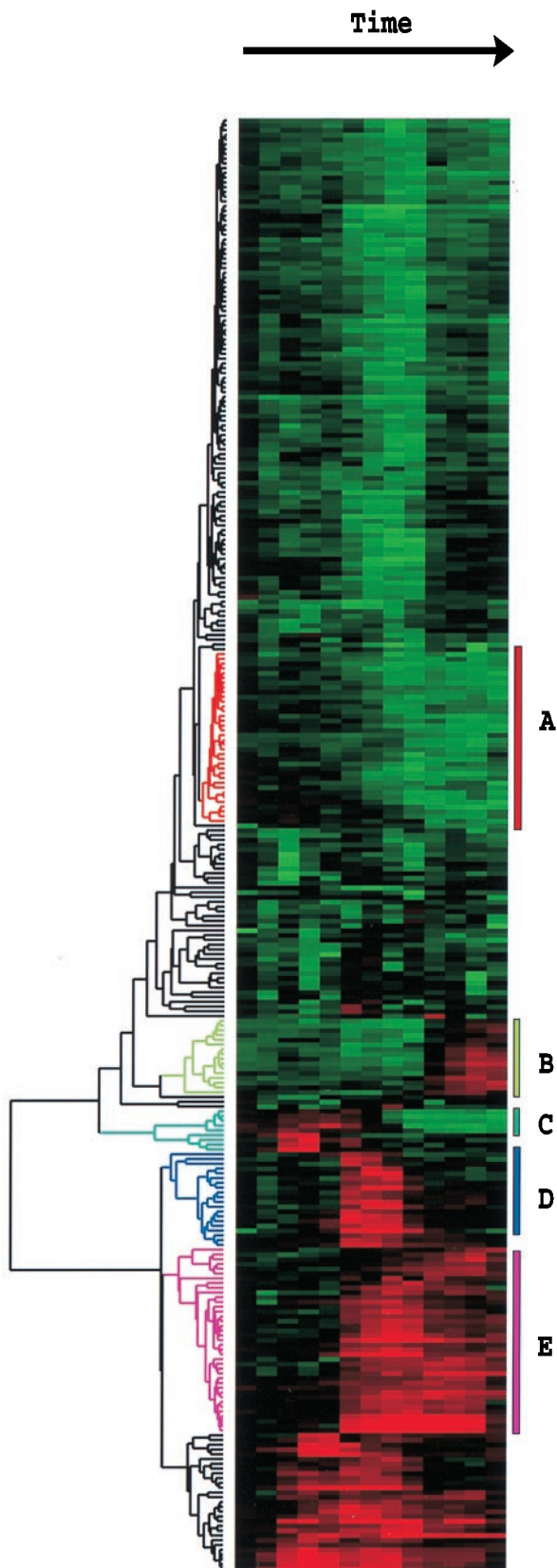


FIG. 1. Clustered display of data from time course of serum stimulation of primary human fibroblasts. Experimental details are described elsewhere (11). Briefly, foreskin fibroblasts were grown in culture and were deprived of serum for 48 hr. Serum was added back and samples taken at time 0, 15 min, 30 min, 1 hr, 2 hr, 3 hr, 4 hr, 8 hr, 12 hr, 16 hr, 20 hr, 24 hr. The final datapoint was from a separate unsynchronized sample. Data were measured by using a cDNA microarray with elements representing approximately 8,600 distinct

regulation. Finally, this result also indicates that noise present in single observations does not contribute significantly when genes are compared across even a relatively small number of nonidentical conditions. Therefore, when designing experiments, it may be more valuable to sample a wide variety of conditions than to make repeat observations on identical conditions.

Genes of Similar Function Cluster Together. A far more striking result is found when larger groups of clustered genes are examined, where we observe a strong tendency for these genes to share common roles in cellular processes. This relationship is clearest in data from experiments on the budding yeast *S. cerevisiae*, where arrays representing essentially all of the genes from this organism are available (8) and for which a large fraction of the identified genes (more than 35%) have been studied in some detail. Fig. 2A represents a clustering analysis of 2,467 genes, all the genes that currently have a functional annotation in the *Saccharomyces* Genome Database (12). As can be seen in Fig. 2B–K, numerous groups of coexpressed genes representing diverse expression patterns across the sampled conditions are involved in common cellular processes. Although one might be concerned about the possibility of crosshybridization, it is clear in the examples below that genes of unrelated sequence but similar function cluster tightly together.

A particularly dramatic example is the extensive cluster (shown in Fig. 2I) of 126 genes strongly down-regulated in response to stress (after each of the shocks, at the latter stages of the diauxic shift where glucose levels are diminished, and after transfer to nutrient-limited sporulation media), and which covary throughout the cell cycle. This cluster is dominated by genes encoding ribosomal proteins (112 genes) and other proteins involved in translation (initiation and elongation factors and tRNA synthetases). It has been reported that yeast responds to favorable growth conditions by increasing the production of ribosomes (13) through transcriptional regulation of genes encoding ribosomal proteins (14).

Mitochondrial protein synthesis genes were also expressed concordantly along with a number of genes involved in respiration (Fig. 2F) in a pattern roughly similar to a large cluster of coexpressed genes involved in ATP synthesis (predominantly members of the F1F0 ATPase complex) and oxidative phosphorylation (Fig. 2G). Oxygen-related transcriptional regulation of genes involved in oxygen utilization has been characterized extensively (15).

The genes encoding the bulk of the components of the proteasome (Fig. 2C) and the mini-chromosome maintenance DNA replication complex (Fig. 2J) are also coexpressed. In addition, there are many examples of coexpressed genes that share a common or related function but are not members of large protein complexes, such as genes encoding numerous glycolytic enzymes (Fig. 2E), genes involved in the tricarbox-

human genes. All measurements are relative to time 0. Genes were selected for this analysis if their expression level deviated from time 0 by at least a factor of 3.0 in at least 2 time points. The dendrogram and colored image were produced as described in the text; the color scale ranges from saturated green for log ratios -3.0 and below to saturated red for log ratios 3.0 and above. Each gene is represented by a single row of colored boxes; each time point is represented by a single column. Five separate clusters are indicated by colored bars and by identical coloring of the corresponding region of the dendrogram. As described in detail in ref. 11, the sequence-verified named genes in these clusters contain multiple genes involved in (A) cholesterol biosynthesis, (B) the cell cycle, (C) the immediate-early response, (D) signaling and angiogenesis, and (E) wound healing and tissue remodeling. These clusters also contain named genes not involved in these processes and numerous uncharacterized genes. A larger version of this image, with gene names, is available at <http://rana.stanford.edu/clustering/serum.html>.

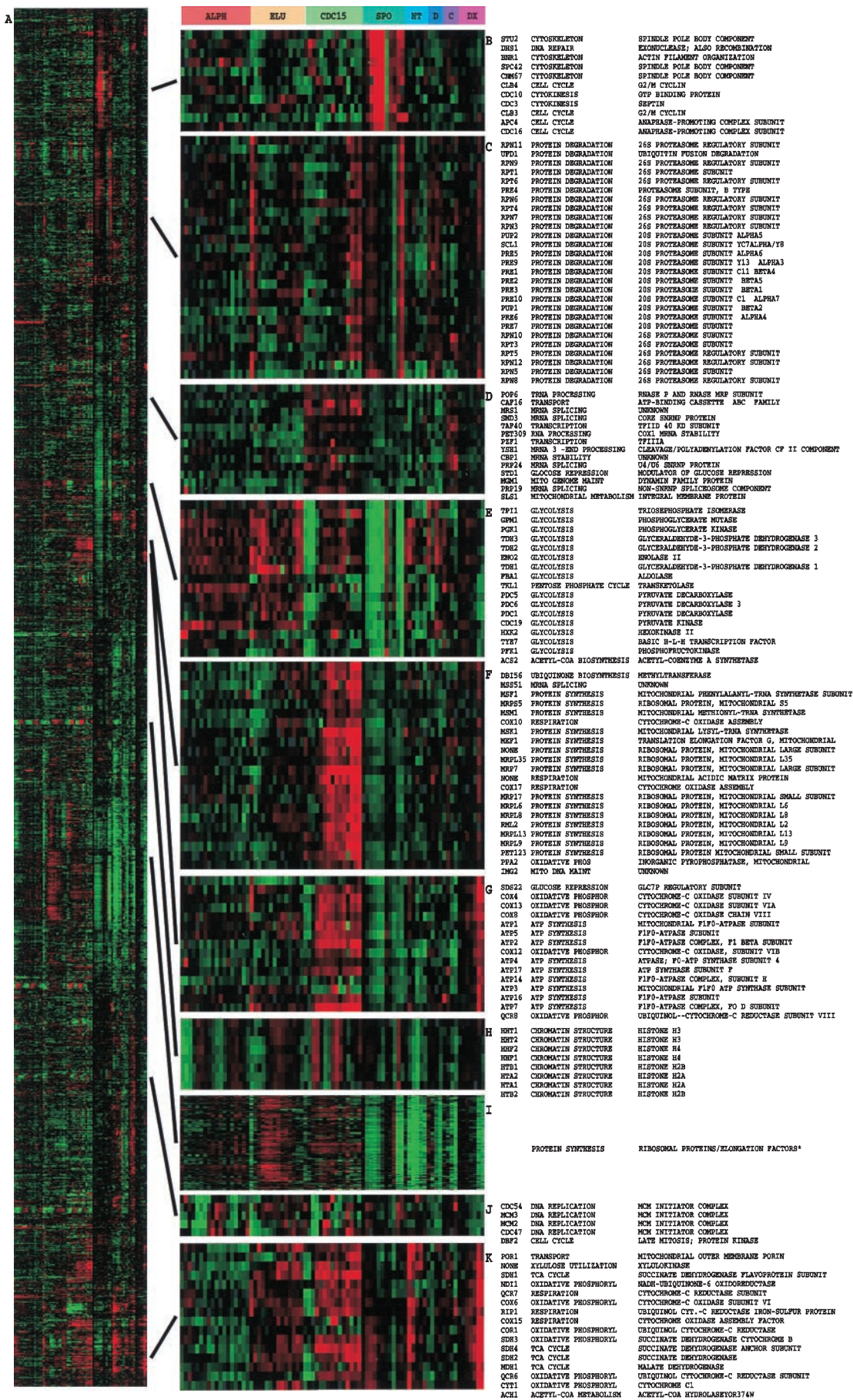


FIG. 2. (Legend appears at the bottom of the opposite page.)

glyc acid cycle and oxidative phosphorylation (Fig. 2K), and genes involved in mating (not shown). These examples emphasize that the observed coregulation occurs primarily at the level of cellular function and not only with the exact protein function (e.g., enzymic reaction catalyzed) of the gene product.

Finally, there is an extremely tight cluster of eight histone genes (duplicates of each of histones H2A, H2B, H3, and H4). It is well known that these genes are coregulated and are transcribed at a particular point in the cell cycle (16).

In human data sets, relationships among the functions of genes in clusters are obscured somewhat by the less complete functional annotation of human gene sequences. Nonetheless, when the composition of the clusters is examined, they are often found to contain genes known to share a common role in the cell. This observation is well illustrated in the data from the response of human tissue culture cells to serum after serum starvation (Fig. 1). When available functional information on the genes studied in this experiment was examined, keeping in mind the often poor state of annotation of the human genome, the clusters of genes indicated by colored branches were found to generally contain genes involved in cholesterol biosynthesis (cluster A), the cell cycle (cluster B), the immediate-early response (cluster C), signaling and angiogenesis (cluster D), and tissue remodeling and wound healing (cluster E); a detailed description of these observations is contained in ref. 11.

DISCUSSION

Microarray-based genomic surveys and other high-throughput approaches (ranging from genomics to combinatorial chemistry) are becoming increasingly important in biology and chemistry. As a result, we need to develop our ability to “see” the information in the massive tables of quantitative measurements that these approaches produce. Our approach to this problem can be generalized as follows. First, we use a common-sense approach to organize the data, based on order inherent in the data. Next, recognizing that the rate-limiting step in exploring and searching large tables of numerical data is a trivial one: reading the numbers (human brains are not well adapted to assimilating quantitative data by reading digits), we represent the quantitative values in the table by using a naturalistic color scale rather than numbers. This alternative encoding preserves all the quantitative information, but transmits it to our brains by way of a much higher-bandwidth channel than the “number-reading” channel.

A natural way of viewing complex data sets is first to scan and survey the large-scale features and then to focus in on the interesting details. What we have found to be the most valuable feature of the approach described here is that it allows this natural and intuitive process to be applied to genomic data sets. The approach is a general one, with no inherent specificity

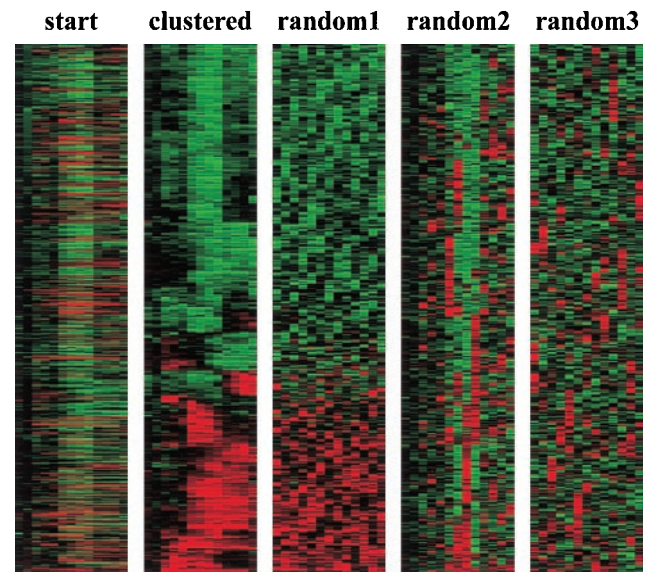


FIG. 3. To demonstrate the biological origins of patterns seen in Figs. 1 and 2, data from Fig. 1 were clustered by using methods described here before and after random permutation within rows (random 1), within columns (random 2), and both (random 3).

to the particular method used to acquire data or even to gene-expression data. It is therefore likely that very similar approaches may be applied to many other kinds of very large data sets. In each case, it may be necessary to find alternative algorithms and computation methods to bring out inherent structures in the data, and, equally important, to find dense naturalistic visual representations that convey the quantitative information effectively. We recognize that the particular clustering algorithm we used is not the only, or even the best, method available. We have used and are actively exploring alternatives such as parametric ordering of genes (9) and supervised clustering methods based on representative hand-picked or computer-generated expression profiles (10). The success of these very simple approaches has given us confidence to face the coming flood of functional genomic data.

The examples presented here demonstrate a feature of gene expression that makes these methods particularly useful, namely the tendency of expression data to organize genes into functional categories. It is, of course, not very surprising that genes that are expressed together share common functions. Nonetheless, the extent to which gene expression patterns suffice to separate genes into functional categories across a relatively small and redundant collection of conditions is surprising. It seems likely that the addition of more and diverse conditions can only enhance these observations. When the clustering analysis described here is

FIG. 2. (On the opposite page.) Cluster analysis of combined yeast data sets. Data from separate time courses of gene expression in the yeast *S. cerevisiae* were combined and clustered. Data were drawn from time courses during the following processes: the cell division cycle (9) after synchronization by alpha factor arrest (ALPH; 18 time points); centrifugal elutriation (ELU; 14 time points), and with a temperature-sensitive *cdc15* mutant (CDC15; 15 time points); sporulation (10) (SPO, 7 time points plus four additional samples); shock by high temperature (HT, 6 time points); reducing agents (D, 4 time points) and low temperature (C; 4 time points) (P. T. S., J. Cuoco, C. Kaiser, P.O. B., and D. B., unpublished work); and the diauxic shift (8) (DX, 7 time points). All data were collected by using DNA microarrays with elements representing nearly all of the ORFs from the fully sequenced *S. cerevisiae* genome (8); all measurements were made against a time 0 reference sample except for the cell-cycle experiments, where an unsynchronized sample was used. All genes (2,467) for which functional annotation was available in the *Saccharomyces* Genome Database were included (12). The contribution to the gene similarity score of each sample from a given process was weighted by the inverse of the square root of the number of samples analyzed from that process. The entire clustered image is shown in A; a larger version of this image, along with dendrogram and gene names, is available at <http://rana.stanford.edu/clustering/yeastall.html>. Full gene names are shown for representative clusters containing functionally related genes involved in (B) spindle pole body assembly and function, (C) the proteasome, (D) mRNA splicing, (E) glycolysis, (F) the mitochondrial ribosome, (G) ATP synthesis, (H) chromatin structure, (I) the ribosome and translation, (J) DNA replication, and (K) the tricarboxylic acid cycle and respiration. The full-color range represents log ratios of -1.2 to 1.2 for the cell-cycle experiments, -1.5 to 1.5 for the shock experiments, -2.0 to 2.0 for the diauxic shift, and -3.0 to 3.0 for sporulation. Gene name, functional category, and specific function are from the *Saccharomyces* Genome Database (13). Cluster I contains 112 ribosomal protein genes, seven translation initiation or elongation factors, three tRNA synthetases, and three genes of apparently unrelated function.

applied to all of the approximately 6,200 genes of *S. cerevisiae*, the clusters of functionally related genes are maintained, but are usually expanded with the addition of uncharacterized genes (the results of this analysis will be the subject of a subsequent report). On the basis of our observations here, it is probable that many of these genes will also share common functions. While not based on biological necessity, similarity of pattern of expression may be the easiest available means of making at least provisional attribution of function on a genomic scale.

Finally, the functional concordance of coexpressed genes imparts biological significance to the broad patterns seen in images like those of Figs. 1 and 2. For example, the representation of the transcriptional response of human fibroblasts to serum shown in Fig. 1 is not simply a list of genes and their associated expression patterns, nor is it an arbitrary structure that is being seen, but rather it is a comprehensive representation of the state of the cell throughout its response to serum. Likewise, for yeast experiments, information on the state of many cellular processes can be inferred quickly by combining and comparing new experiments with the data presented here.

We thank J. De Risi for excellent technical assistance and many useful suggestions and the staff of the *Saccharomyces* Genome Database. We also thank J. Cuoco and C. Kaiser for the use of unpublished results. This work was supported by a grants from the National Institutes of Health (GM 46406, HG 00983, and CA77097). P.O.B. is an associate investigator with the Howard Hughes Medical Institute. P.T.S. was supported by a training grant from the National Eye Institute (Bethesda, MD). M.B.E. was supported by a postdoctoral fellowship from the Alfred E. Sloan Foundation (New York, NY).

1. Schena, M., Shalon, D., Davis, R. W. & Brown, P. O. (1995) *Science* **270**, 467–470.
2. Velculescu, V. E., Zhang, L., Vogelstein, B. & Kinzler, K. W. (1995) *Science* **270**, 484–487.
3. Lockhart, D. J., Dong, H., Byrne, M. C., Follettie, M. T., Gallo, M. V., Chee, M. S., Mittmann, M., Wang, C., Kobayashi, M., Horton, H., *et al.* (1996) *Nat. Biotechnol.* **14**, 1675–1680.
4. Kohonen, T. (1997) *Self-Organizing Maps* (Springer, New York).
5. Sokal, R. R. & Michener, C. D. (1958) *Univ. Kans. Sci. Bull.* **38**, 1409–1438.
6. Schena, M., Shalon, D., Heller, R., Chai, A., Brown, P. O. & Davis, R. W. (1996) *Proc. Natl. Acad. Sci. USA* **93**, 10614–10619.
7. Shalon, D., Smith, S. J. & Brown, P. O. (1996) *Genome Res.* **6**, 639–645.
8. DeRisi, J. L., Iyer, V. R. & Brown, P. O. (1997) *Science* **278**, 680–686.
9. Spellman, P. T., Sherlock, G., Iyer, V. R., Zhang, M., Anders, K., Eisen, M. B., Brown, P. O., Botstein, D. & Futcher, B. (1998). *Mol. Biol. Cell*, in press.
10. Chu, S., DeRisi, J., Eisen, M., Mulholland, J., Botstein, D., Brown, P. O. & Herskowitz, I. (1998) *Science* **282**, 699–705.
11. Iyer, V. R., Eisen, M. B., Ross, D. R., Schuler, G., Moore, T., Lee, J. C. F., Trent, J. M., Hudson, J., Boguski, M., Lashkari, D., *et al.* (1998) *Science*, in press.
12. Cherry, J. M., Ball, C., Weng, S., Juvik, G., Schmidt, R., Adler, C., Dunn, B., Dwight, S., Riles, L., Mortimer, R. K., *et al.* (1997) *Nature (London)* **387**, 67–73.
13. Kief, D. R. & Warner, J. R. (1981) *Mol. Cell. Biol.* **1**, 1007–1015.
14. Kraakman, L. S., Griffioen, G., Zerp, S., Groeneveld, P., Thevelein, J. M., Mager, W. H. & Planta, R. J. (1993) *Mol. Gen. Genet.* **239**, 196–204.
15. Kwast, K. E., Burke, P. V. & Poyton, R. O. (1998) *J. Exp. Biol.* **201**, 1177–1195.
16. Hereford, L. M., Osley, M. A., Ludwig, T. R. 2nd. & McLaughlin, C. S. (1981) *Cell* **24**, 367–375.